Journal of Energy Storage 134 (2025) 118161

Contents lists available at ScienceDirect

Journal of Energy Storage

journal homepage: www.elsevier.com/locate/est

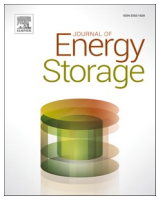

Research papers

Experimental analysis of AB_2 metal hydride storage in PEM power-to-hydrogen systems: Integration and energy trade-offs

Riccardo Alleori [a], Maria Alessandra Ancona [b], Michele Bianchi [b], Francesco Falcetelli [b], Federico Ferrari [b,*], Paolo Pilati [c]

[a] Alma Mater Studiorum Università di Bologna, Inter-Departmental Center for Industrial Research on Renewable Sources, Environment, Sea and Energy (CIRI-FRAME), Via Terracini 24, 40131 Bologna, Italy
[b] Alma Mater Studiorum Università di Bologna, Department of Industrial Engineering (DIN), Viale del Risorgimento 2, 40136 Bologna, Italy
[c] Alma Mater Studiorum Università di Bologna, Department of Electrical, Electronic and Information Engineering (DEI), Viale del Risorgimento 2, 40136 Bologna, Italy

ARTICLE INFO

Keywords:
Hydrogen storage
Metal hydrides
Experimental set-up
Power-to-gas
Electrolyzer-storage interaction

ABSTRACT

The integration of hydrogen storage into renewable energy systems demands diversified technological solutions to address the inherent intermittency of renewable power. In this context, low-pressure metal hydride (MH) systems offer a compelling alternative to high-pressure hydrogen storage systems, particularly in applications with stringent safety requirements or spatial limitations. Their reversible absorption characteristics and solid-state storage capabilities position them as a valuable option within the broader hydrogen storage landscape. This study presents experimental results and an energy-focused analysis evaluating the thermodynamic behavior and efficiency of MH-based storage modules operating within a Power-to-Gas configuration. The work investigates how pressure and thermal management affect the trade-off between energy efficiency and renewable energy utilization. Findings indicate that operation at 15 bar with passive thermal regulation (20 °C without active cooling) enables high hydrogen uptake, limits energy losses, and ensures a balanced system response. This configuration proves especially relevant in real-world scenarios prioritizing safety, simplicity, and renewable energy absorption.

1. Introduction

The transition toward a sustainable energy paradigm necessitates the deployment of safe, efficient, and scalable energy storage systems capable of mitigating the intermittency of renewable energy sources. In this context, hydrogen is widely recognized as a promising energy vector due to its high energy density and zero-carbon emissions at the point of use. However, storage remains one of the main technical and economic hurdles to its widespread adoption. Conventional storage methods—such as high-pressure compression or cryogenic liquefaction—impose high energy costs and raise safety concerns, particularly in densely populated or urban areas [1].

To overcome these limitations, metal hydrides (MHs) have emerged as a compelling alternative, especially in stationary applications such as Power-to-Gas (P2G) systems. Their ability to reversibly absorb and desorb hydrogen under moderate pressure and temperature conditions makes them particularly suitable for safe and compact storage. Compared to compressed or liquefied hydrogen, MHs offer higher volumetric hydrogen densities and improved safety profiles [2]. Among them, AB_2-type intermetallic hydrides stand out for their favorable thermodynamic properties, tunable equilibrium pressures, and relatively fast sorption kinetics [2]. Nonetheless, challenges such as kinetic limitations, thermal management, and material degradation over cycling persist and remain active areas of research. Recent advances in nanostructuring and alloy design have shown promise in enhancing both sorption kinetics and long-term stability [3].

In parallel with material development, numerical and experimental studies have highlighted the importance of thermal management in MH systems. For example, Bhogilla [4] simulated a cylindrical AB_2-based hydride tank, demonstrating how the geometry of internal heat exchangers significantly impacts absorption/desorption rates and storage reversibility. Their results underscored that maintaining uniform temperature profiles is crucial for system responsiveness, especially when operating under intermittent renewable inputs.

From a safety perspective, MHs present significant advantages: hydrogen is stored in solid form at low pressures, thereby reducing risks

* Corresponding author.
E-mail address: federico.ferrari28@unibo.it (F. Ferrari).

https://doi.org/10.1016/j.est.2025.118161
Received 5 June 2025; Received in revised form 29 July 2025; Accepted 19 August 2025
Available online 28 August 2025

associated with leaks, flammability, or high-pressure vessel failure. This makes them well-suited for stationary storage in residential or urban settings, where stringent safety regulations apply [5].

In stationary hydrogen storage systems, weight is generally not a limiting factor, allowing MHs to fully exploit their high volumetric density and compactness. This feature is particularly valuable in off-grid systems, where low-pressure operation enhances safety and ease of maintenance, as well as in grid-connected environments, where space efficiency is essential [6]. Another important advantage of MH-based systems is their ability to decouple energy and power scaling: unlike batteries, where increasing capacity also requires additional power electronics, MH systems can be scaled in energy simply by enlarging the storage tank. This design flexibility makes them particularly attractive for large-scale and long-duration storage applications [6]. Moreover, MHs also open the door to chemical hydrogen compression, offering solid-state, low-temperature alternatives to conventional mechanical compressors, which often suffer from complexity, noise, and leakage [7].

Several recent studies reinforce the techno-economic potential of MHs in P2G and hydrogen energy systems. Their high energy density, compactness, and ability to exploit waste heat for hydrogen desorption make them ideal for integrated energy storage [8]. For instance, Wang et al. [9] performed a comprehensive analysis showing that systems based on $TiFe_{0.85}Mn_{0.05}$ and similar hydrides can reach levelized costs of storage (LCOS) as low as 0.383 $/kWh, outperforming conventional 170-bar compressed gas systems in both cost and land use. Similarly, Lototskyy et al. [10] highlighted the robustness and safety of MHs for stationary gas-phase applications, while Franke and Kazula [11] explored their potential in sustainable aviation, underlining the possibility of lightweight and safe onboard storage.

However, the actual performance of MH systems remains sensitive to dynamic operating conditions. Charging and discharging rates directly influence sorption behavior and system economics, meaning that competitiveness depends not only on material cost but also on efficient integration with upstream units such as electrolyzers [9]. In this regard, electrolyzer operating parameters—such as current density and cell voltage—are critical: lower voltages improve energy efficiency, while higher current densities can reduce capital costs by minimizing the number of required cells [12].

In recent years, several demonstration projects have successfully integrated MH storage with renewable energy sources and fuel cells, validating their feasibility in microgrids, standalone residential units, and even commercial buildings [13–15]. In parallel, within the broader Power-to-X framework, metal hydrides have been used not only for storage but also as part of integrated pathways that convert surplus renewable energy into synthetic hydrocarbons through downstream catalytic processes [16]. These successful deployments illustrate the technological readiness of MHs but also highlight the remaining challenges in moving from demonstrator to commercial maturity. Chief among them are the needs for optimized thermal control and tight system-level integration, particularly under fluctuating renewable inputs. In these scenarios, MHs have proven to be a robust solution for long-duration energy storage, serving as a complementary technology to batteries, which are more suitable for short-term balancing [6].

Despite the extensive literature on MHs, most studies focus on material-level or component-level analyses, while integrated system assessments remain relatively scarce. This work addresses that gap by evaluating the integration of an AB_2-type metal hydride storage system with a commercial electrolyzer in a stationary Power-to-Hydrogen configuration. To this end, an experimental test bench was developed to investigate system behavior under variable operating conditions, representative of real-world renewable scenarios. An energy analysis was also conducted to evaluate system-level efficiency, enabling the development of empirical correlations to support future design optimization and retrofitting strategies.

Although rigorous methods exist for deriving the thermodynamic and kinetic properties of MHs – such as the precise PCT isotherm approach proposed by Rodriguez et al. [17] – this study adopts a more application-oriented perspective. Given that the exact alloy composition used in the experiments is confidential, an empirical estimation of the hydride's thermodynamic behavior was derived from limited Van't Hoff data and cross-validated with authoritative sources [7,18]. This approximation is deemed sufficient for the purpose of system integration, where the priority lies in evaluating overall performance, rather than detailed material characterization.

Beyond technical assessment, special attention was given to the trade-off between energy efficiency and capacity utilization, which is often overlooked in traditional analyses. In renewable-driven Power-to-Hydrogen systems, maximizing efficiency alone does not guarantee optimal exploitation of surplus energy. Therefore, this study aims to clarify how different operating strategies affect both process efficiency and the system's ability to absorb intermittent renewable inputs - a key requirement for practical deployment. Preliminary experimental results provide new insights into the thermodynamic behavior of MHs under dynamic conditions, which may inform the development of empirical models, improve integration with renewables, and support adaptive operating strategies depending on the functional objectives - whether they be efficiency maximization or renewable energy absorption.

2. Materials and methods

This study employs an experimental and analytical methodology to characterize the performance of a metal hydride-based hydrogen storage system in direct coupling with a Proton Exchange Membrane (PEM) electrolyzer. Unlike conventional storage configurations that require intermediate compression stages, this configuration allows hydrogen absorption directly at the output pressure of the electrolyzer, thus minimizing energy losses and simplifying system integration.

As detailed in the following paragraphs, the methodology section can be divided into three main parts: (*i*) the experimental setup description, illustrating the custom-built test bench, where the electrolyzer and metal hydride canisters dynamically interact under varying operating conditions; (*ii*) the Design of Experiments (DoE) definition, outlining the systematic variation of temperature and pressure across multiple levels to assess their influence on hydrogen adsorption and desorption; and (*iii*) the energy assessment, defining and evaluating the system's efficiency as the product of individual components efficiencies, with a focus on the impact of direct coupling between the electrolyzer and the metal hydride canisters on energy performance. This integrated approach provides critical insights into the thermodynamic and kinetic behavior of commercial metal hydride canisters under real-world operating conditions.

2.1. Experimental setup and procedure

The experimental test bench, schematized in Fig. 1, consists of a P2G system in which a PEM electrolyzer (PEM-E) is directly coupled with MH canisters of two different sizes for hydrogen storage. Since hydrogen adsorption in MH is an exothermic process, an integrated thermal conditioning system is included to actively control the canisters' temperature during charging and discharging phases.

In detail, the experimental setup is composed of the following key components:

i. a PEM-E able to produce 44.5 g/h (500 NL/h) of hydrogen at 15 bar. The electrolyzer is characterized by a nameplate input power equal to 2.5 kW AC and by an average efficiency of around 60 % (on lower heating value (LHV) basis);
ii. two MH canisters (AB_2) of different sizes:
    a. a cylindrical 0.6 Nm^3 canister, able to store around 54 g of hydrogen at 30 bar within an internal volume of 1.4 L (~1.28 kWh/L on LHV);

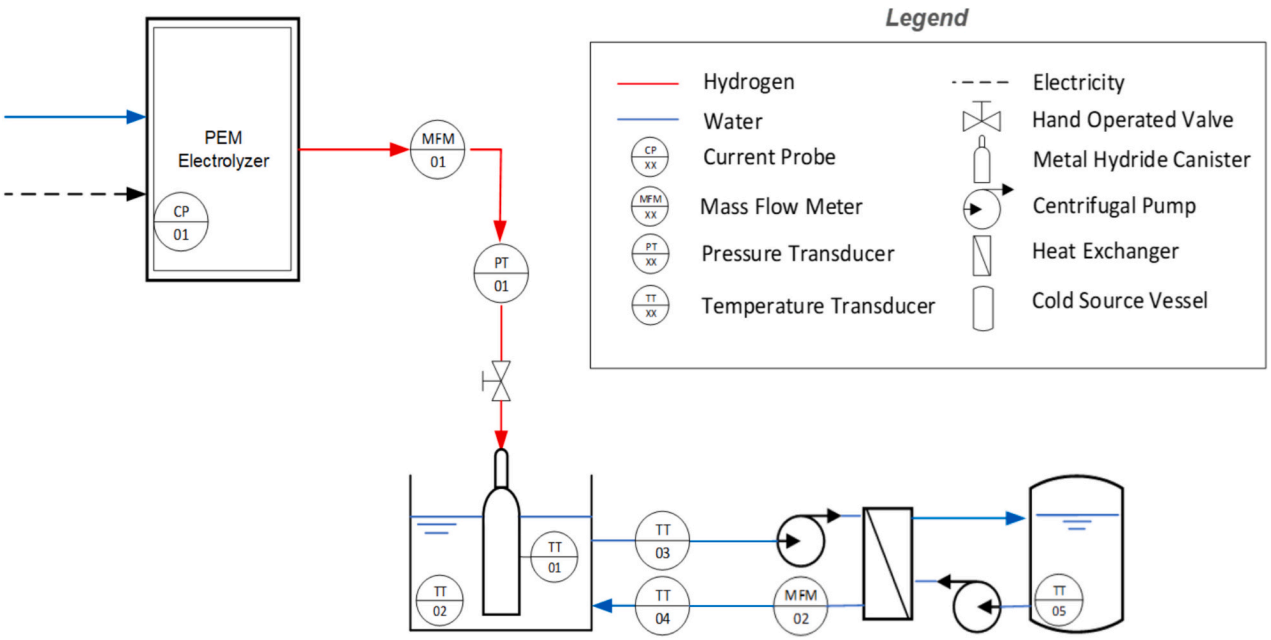

Fig. 1. P&ID of the considered test bench.

b. a cylindrical 0.9 Nm^3 canister, able to store 81 g of hydrogen at 30 bar within an internal volume of 1.7 L (~1.58 kWh/L on LHV);

iii. a closed-loop water cooling circuit designed to regulate the canisters' temperature. It includes a centrifugal water pump, a thermal buffer tank, and a water-bath heat exchanger to enhance heat dissipation during hydrogen adsorption;

iv. a Data Acquisition and Control (DAQC) system incorporating a Python™-based GUI for real-time data visualization and control. The system communicates *via* TCP/IP and Modbus protocols, enabling seamless integration with Arduino™ microcontrollers, the electrolyzer's Programmable Logic Controller (PLC), and a Pico Technology TC-08 thermocouple data logger for precise temperature measurements. The system is fully instrumented with pressure, temperature, flow, and weight sensors (electronic scale, max 16 kg ± 0.1 g) for a detailed characterization of the hydrogen storage process.

A summary of the measurement points, the installed sensors, and their characteristics is given in Table 1.

Fig. 2, instead, provides a detailed depiction of the experimental test bench in its current configuration.

This setup offers a robust framework for assessing the thermodynamic and kinetic behavior of the MH storage system under various operating conditions, ensuring reproducibility and precise measurement accuracy.

Specifically, the hydrogen adsorption by the metal alloy is quantified by integrating the hydrogen flow rate entering the canisters over time, as measured by a flow meter located on the feed line between the electrolyzer and the canister. The working pressure within the hydrogen feed branch is determined by the pressure increase within the hydride cylinder and it is continuously monitored by a pressure sensor positioned at the cylinder's head.

In addition, to account for temperature variations resulting from the exothermic nature of adsorption, three thermocouples are affixed to the cylindrical surface of the storage vessel. These thermocouples monitor the thermal profile during the dynamic characterization phase. Additionally, a circulating water-cooling system is employed to extract and quantify the thermal power dissipated by the cylinder during the charging process.

2.2. Design of experiments

To systematically assess the performance of the MH storage system in direct coupling with a PEM electrolyzer, the experimental campaign was structured following a DoE approach. Specifically, a 2 × 2 factorial design was implemented for each MH canister, resulting in two separate experimental matrices – Table 2. Each matrix explores the system behavior over two different levels of temperature and pressure, allowing a comprehensive mapping of hydrogen absorption dynamics under realistic operating conditions.

The objective of this DoE is to identify the key performance trends and provide practical guidelines for correctly sizing a P2G system based on MH storage. By systematically varying the operating conditions, the study aims to define the optimal pressure-temperature configurations that maximize system efficiency while ensuring reliable and safe operation.

By assessing the performance of commercial MH storage under these conditions, this study delivers engineering insights to support the direct coupling of PEM electrolyzers with MH storage, facilitating scalable and efficient hydrogen-based energy solutions.

Table 1
Measured physical quantities and corresponding installed sensors.

Physical quantity	Symbol	Unit	Sensor	Accuracy	Measuring range	Output signal
H_2 delivery pressure	p_{H2}	bar	Pressure transducer	±0.25 FS	0 ÷ 15	0 ÷ 10 V
H_2 delivery mass flow	$\dot{m}_{H2}$	NL/min	Thermal mass flow meter	±0.5 % FS	0.1 ÷ 15	0 ÷ 5 V
Temperatures	T	°C	T-type thermocouple	±0.5 °C	−20 ÷ 350	TC
Current	I	A	DC/AC current probe	±4 % measure + 50 mA	0 ÷ 100	100 mV/A
H_2O mass flow	$\dot{m}_{H2O}$	L/s	Electromagnetic flow meter	±0.5 % RV	0 ÷ 9.8	4–20 mA

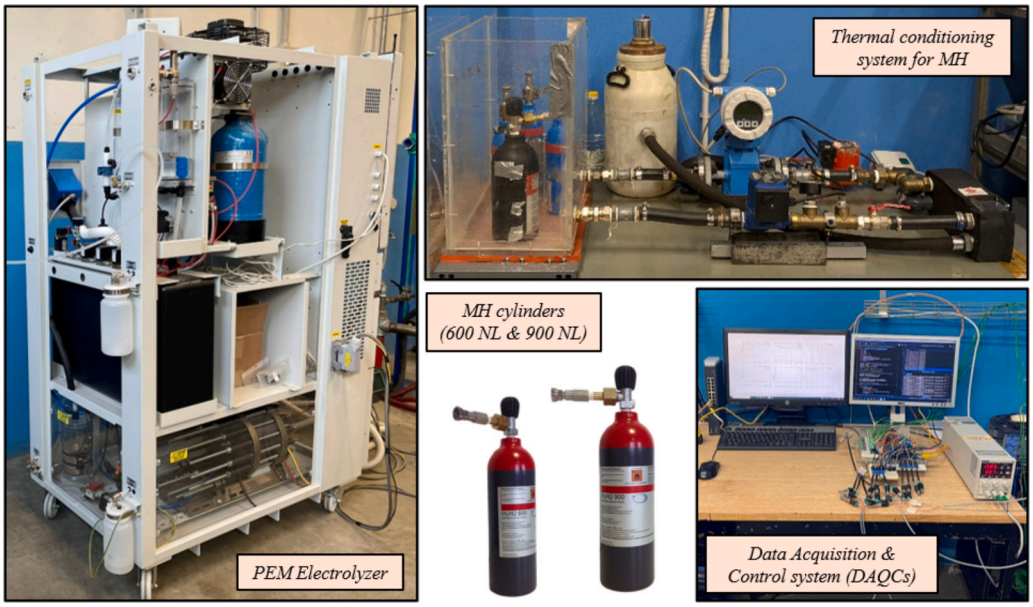

Fig. 2. Test bench sections and components.

Table 2
Design of experiments.

	Temperature (°C)	
	20 °C	30 °C
Pressure (bar)		
7 bar	Case 1	Case 2
15 bar	Case 3	Case 4

2.3. Energy and efficiency assessment

An extensive energy analysis was conducted to evaluate the performance of the system under various operating conditions. The hydrogen mass produced and stored was determined by integrating the measured flow rates over time during the electrolyzer operation and MH charging phases.

$$m_{H2} = \int_0^t \rho_{H2} \bullet \dot{V}_{H2} dt \tag{1}$$

where ρ_{H2} is the hydrogen density [kg/m^3], $\dot{V}_{H2}$ is the flow rate of hydrogen sent by the electrolyzer to the canisters [NL/s] and t is the time [s].

Furthermore, taking into account the exothermic behavior of MHs during hydrogen absorption, the equivalent electrical energy consumption of a chiller required to cool the MH system and maintain optimal storage conditions was calculated as follows:

$$E_{th,MH} = n_{H2} \cdot \Delta H_{MH} \tag{2}$$

$$Q_{cool} = \int_0^t \dot{V}_{H2O} \rho_{H2O} c_l \Delta T \, dt \tag{3}$$

$$E_{cool} = \frac{Q_{cool}}{EER} \tag{4}$$

where n_{H2} is the number of hydrogen moles [mol], ΔH_{MH} is the enthalpy of formation [J/mol], $\dot{V}_{H2O}$ is the volumetric flow rate of cooling water [m^3/s], ρ_{H2O} is water density [kg/m^3], c_l is the water specific heat [J/kgK], ΔT is the temperature difference between inlet and outlet of the water bath [K] while *EER* is the Energy Efficiency Ratio of the chiller [−], assumed equal to 3.

By combining these calculations with the experimentally monitored electrical consumption of the electrolyzer, the overall P2G efficiency and the storage efficiency of the MH system were assessed:

$$\eta_{P2G} = \frac{m_{H2} \cdot LHV}{E_{stack} + E_{aux} + E_{cool}} \tag{5}$$

$$\eta_{storage} = 1 - \frac{Q_{cool}}{m_{H2} \cdot LHV} \tag{6}$$

where *LHV* is the Lower Heating Value of hydrogen [kWh/kg], E_{stack} and E_{aux} are respectively the energy consumption of the PEM stack and of its Balance of Plant (BoP) [kWh].

In addition, to ensure the optimal performance of a P2G plant, it is crucial to properly size the electrolyzer-to-MH storage ratio, particularly when the system is coupled with renewable energy sources (RES). In this regard, it is useful to define the Capacity Factor (*CF*) for a plant as the measure of how effectively the plant operates relative to its maximum potential output (concerning the maximum hydrogen production of the electrolyzer) over a given period:

$$CF = \frac{\text{Actual Energy Output Over a Period}}{\text{Maximum Possible Energy Output Over the Same Period}} \cdot 100\% \tag{7}$$

Given that the *CF* of the electrolyzer depends on the availability of renewable power and the ability to store produced hydrogen efficiently, the hydrogen absorption rates of MH storage systems impose constraints that must be considered in the system design. If the MH system cannot absorb hydrogen at a rate matching the electrolyzer output, production may need to be curtailed, reducing the effective *CF* of the electrolyzer and, consequently, the overall P2G plant. Conversely, oversizing the MH storage without adequate hydrogen production capacity could lead to underutilization and increased system costs. Therefore, an optimal balance must be achieved to align the electrolyzer hydrogen output with the MH system's absorption kinetics, ensuring continuous operation and maximizing the *CF* of the integrated P2G system. This is especially critical in renewable-driven configurations, where intermittent energy supply further complicates the system's dynamic response.

Since P2G are composed of multiple energy systems (*i.e.*, photovoltaic, wind, *etc.*), it is possible to calculate the *CF* for a facility considering the weight of each source contribution:

$$CF_{facility} = \frac{\sum (P_i \times CF_i)}{\sum P_i} \quad (8)$$

where CF_i, is the capacity factor of each power source, and P_i, is the installed capacity of each power source.

If the electrolyzer operates only when renewable energy is available, its effective *CF* will be dictated by the availability of excess renewable power. If battery storage is present, it can smooth out fluctuations and increase the effective *CF*. Curtailment losses must be considered, especially when wind and solar peak simultaneously but exceed the electrolyzer capacity.

Reasonable values of *CF* for LT-P2G systems could be as follows [19]:

- 30÷50 % for systems integrated with variable renewable energy sources (*e.g.*, wind, solar);
- 60÷80 % for P2G plants with stable renewable electricity supply (*e.g.*, nuclear, hydro);
- higher than 80 % in fully optimized grid-connected settings with continuous electricity availability.

Therefore, to accurately determine the optimal size ratio between the electrolyzer and MH storage, it is essential to explore all operational boundaries, including MH temperature, hydrogen supply pressure, and their impact on direct coupling dynamics. These parameters significantly influence the hydrogen absorption/desorption rates, which in turn affect the overall system efficiency and *CF* of the P2G plant. Additionally, the role of the BoP must be carefully assessed, as auxiliary components and control systems can introduce additional energy demands and operational constraints. A comprehensive evaluation of these factors is crucial not only from a technical perspective but also from an economic standpoint, as it allows for a more precise estimation of the cost-effectiveness of integrating MH storage compared to traditional high-pressure (HP) hydrogen storage. By thoroughly analyzing these interdependencies, it becomes possible to design a P2G system that maximizes efficiency, minimizes losses, and ensures a sustainable and economically viable hydrogen storage solution. This methodology enabled the quantification of the impact of different operating conditions—such as supply pressure, MH temperature, and charging rates—on system performance, providing key insights into the energy efficiency and feasibility of integrating MH storage within a P2G framework.

3. Results and discussion

In this section, the thermodynamic results obtained from the experimental campaign are presented and analyzed, providing key insights into the performance of the MH storage system under different operating conditions. Particular attention is given to the direct coupling between the PEM-E and the MH storage, highlighting its impact on hydrogen absorption dynamics, system efficiency, and overall storage capacity. The discussion aims to interpret the observed trends, assess the influence of key parameters such as supply pressure and thermal conditioning, and identify potential optimization strategies for enhancing system integration. These findings serve as a foundation for future developments in the design and management of P2H systems.

3.1. Data-informed estimation procedure for MH key parameters

Given that the experimental investigation was conducted using commercial AB_2-type storage cylinders, comprehensive data regarding the physicochemical properties and composition of the metal alloy were not available, as well as the complete geometrical data for each device.

The precise chemical composition of the metal hydride alloy contained in the canisters used in this study is not disclosed by the manufacturer due to confidentiality constraints. However, according to the safety data sheet (SDS) provided, the alloy belongs to the AB_2-type intermetallic class, which is commonly employed in reversible hydrogen storage systems due to its favorable thermodynamic and kinetic properties. The SDS provides the approximate weight percentages of the constituent elements - namely manganese (40–60 %), titanium (20–40 %), vanadium (10–30 %), zirconium (2.5–7 %), and iron (1.5–3 %) - allowing for a general estimation of the alloy's composition. While the exact stoichiometry remains unknown, the available data enable just to hypothesize a likely formulation consistent with established AB_2 structures.

To address this limitation, an iterative empirical methodology was developed to infer key parameters, including the mass of the metal hydride powder inside the cylinder and that of the confinement system, as well as the enthalpy ΔH and entropy ΔS of formation. Specifically, these parameters were determined through an experimental regression approach, leveraging the Pressure Concentration Temperature (PCT) curves of the metal alloy reported in the manufacturer's datasheet – see Fig. 3 – and those reconstructed on a system-wide basis, considering the weight fraction ($wt\%_{ss}$) of hydrogen storage with respect to the total mass of the device, thereby incorporating the contributions of the confinement structure and valve assembly.

$$wt\%_{ss} = \frac{m_{H2}}{m_{ss}} \cdot 100 \quad (9)$$

where:

$$m_{ss} = m_{H2} + m_{MH} + m_{shell} \quad (10)$$

This methodology ensures a more rigorous and comprehensive characterization of the alloy's thermodynamic properties within the constraints of the available data.

The results obtained through the iterative method are summarized in Table 3.

As previously mentioned, the enthalpy and entropy values for the metal alloy in question were derived using Van't Hoff's equation:

$$\ln\left(\frac{p_{eq}}{p_{ref}}\right) = \frac{\Delta H}{RT} - \frac{\Delta S}{R} \quad (11)$$

where:

- p_{eq} is the equilibrium hydrogen pressure [bar]
- ΔH is the enthalpy change of hydride formation [J/mol]
- R is the universal gas constant equal to 8.314 J/molK
- T is the absolute temperature [K]
- ΔS is the entropy change of hydride formation [J/molK]

The Van't Hoff plot related to the thermodynamic characterization is shown in Fig. 4, while the enthalpy and entropy values for the two phases are summarized in Table 4.

$$\ln\left(\frac{p_{eq}}{p_{ref}}\right) = -3562.5 \cdot \left(\frac{1}{T}\right) + 14.234 \quad (Absorption)$$

$$\ln\left(\frac{p_{eq}}{p_{ref}}\right) = -4139.7 \cdot \left(\frac{1}{T}\right) + 15.612 \quad (Desorption)$$

The reliability of the empirically estimated thermodynamic parameters – namely, the enthalpy (ΔH) and entropy (ΔS) of hydride formation – was evaluated through comparison with established data from the scientific literature on AB_2-type metal hydride alloys for hydrogen storage. Notably, the values derived in this study align closely with those reported in [7,18], both of which present reference datasets for a range of Ti–Fe–Mn-based AB_2 compounds ($\Delta H \approx -30 \pm 10$ kJ/mol H_2, $\Delta S \approx -110 \pm 20$ J/mol•K). The comparison confirms that our estimated values are consistent with materials of similar elemental composition, reinforcing the validity of the thermodynamic assumptions derived from the SDS. Since the primary objective of this study was not the detailed

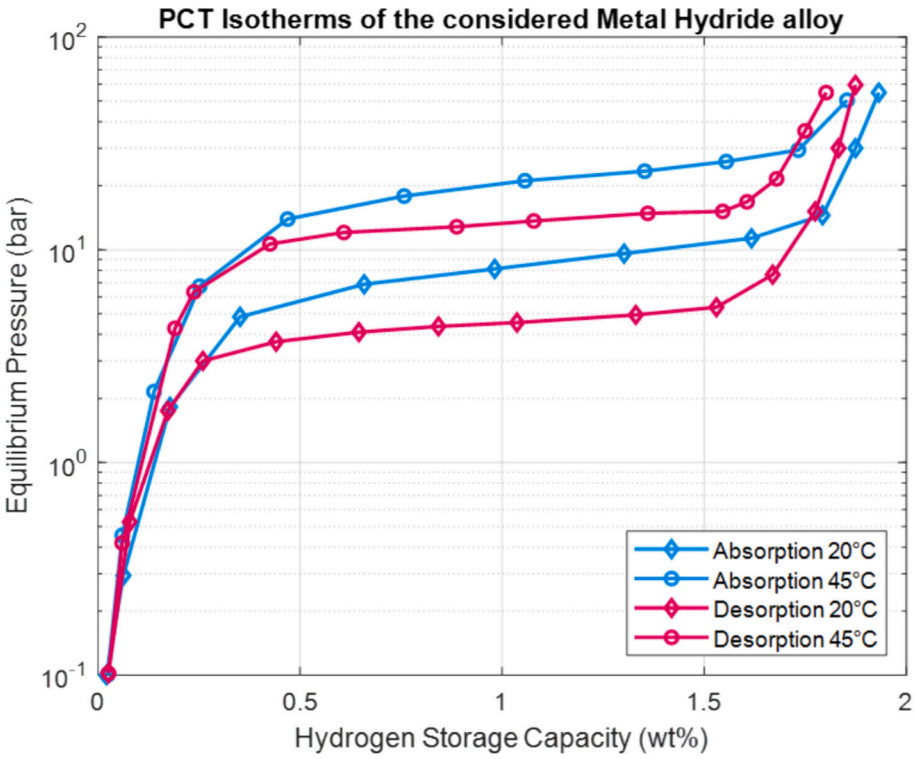

Fig. 3. PCT curves.

Table 3
Results from the iterative regression.

	Mass of empty cylinder	Mass of metal alloy	Mass of canister shell
900 NL	7698.4 g	4250.6 g	3447.8 g
600 NL	5543.6 g	2833.7 g	2709.9 g

chemical characterization of the canister alloy, but rather the assessment of its thermodynamic behavior under working conditions, we considered it sufficient to employ a minimal dataset consisting of two isotherms for constructing the Van't Hoff plot. While additional isotherms would certainly improve the precision of the ΔH and ΔS estimates, the selected approach offers a satisfactory balance between experimental effort and accuracy, especially in light of the strong agreement with established literature benchmarks.

With the experimentally determined enthalpy and entropy values, it was possible to quantify the thermal contribution associated with the absorption phase for each specific operating condition. This was achieved by computing the thermal energy released during hydrogen absorption, case by case, based on the thermodynamic parameters obtained through regression. The calculated thermal loads were then systematically compared with the actual thermal power expended to cool down the storage cylinders during the charging process. This comparison enables an assessment of the efficiency of the cooling system in dissipating the heat generated by the exothermic reaction, providing valuable insights into the thermal management requirements of the storage system.

3.2. Effect of operating conditions on hydrogen storage

For a deeper understanding of the interaction between the PEM-E and MH canisters in a direct coupling configuration, it is essential to analyze the control strategy of the hydrogen generator. The control logic of the PEM-E during the absorption phase is governed by the pressure differential between the production set-point defined by the user and the delivery pressure. As a result, the hydrogen flow rate profile dynamically adapts to the downstream thermodynamic conditions varying linearly with the pressure gap as shown in Fig. 5 It is therefore important to emphasize that the hydrogen absorption flow rate trends presented in the following sections of this document represent the overall behavior of the system and do not solely reflect the intrinsic absorption kinetics of the metal alloy used.

Although each test is deemed complete upon reaching the set-point pressure within the MH canister, the energy analysis was conducted over a standardized time window of 2 h from the start of hydrogen delivery. This approach ensures consistency and comparability across the experimental campaign, allowing for a uniform evaluation of the different operating conditions, irrespective of the specific absorption kinetics observed.

The following sections will present the key trends observed for the most representative cases in evaluating the performance of the P2G system under the operating conditions defined by the DoE. Specifically, the analysis will first focus on the system's behavior as a function of the MH cooling temperature (cases #3 and #4) and then highlight similarities and differences in comparison with cases characterized by different supply pressures (cases #1 and #3), as these have been identified as the most representative scenarios.

3.2.1. Impact of cooling fluid temperature

As shown in Fig. 6, the surface temperature of the cylinder initially rises rapidly before gradually decreasing at a slower rate, due to thermal inertia of the system. As will be discussed later, this effect becomes more pronounced at higher supply pressures, where improved reaction kinetics enhance hydrogen absorption performance. For both storage configurations, it is observed that, at a given supply pressure, as soon as the electrolyzer begins hydrogen delivery, the gas absorption rate by the storage cylinder initially matches the maximum flow rate supplied by the generator – Fig. 6. During this initial stage of the charging process, the absorption rate remains at its peak before progressively declining as the MH approaches saturation, marking the completion of the absorption process – Fig. 6.

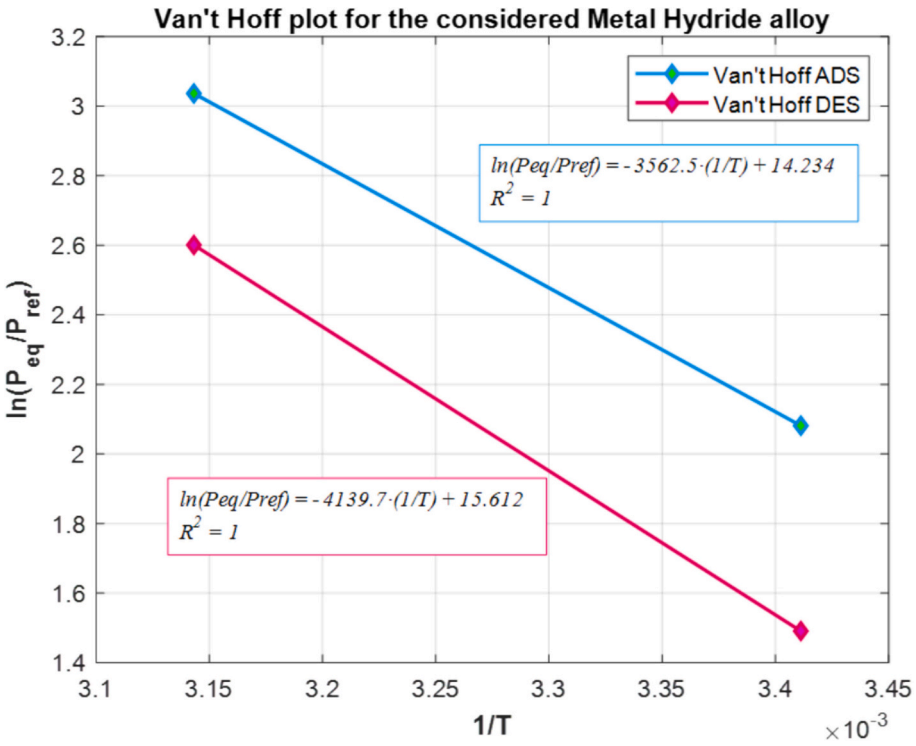

Fig. 4. Van't Hoff curves for the considered MH alloy.

Table 4
Enthalpy and entropy of formation for the considered metal alloy.

Calculation of the enthalpy and entropy of formation			
ADS	ΔH	−29.619	kJ/mol
	ΔS	0.118	kJ/mol·K
DES	ΔH	−34.417	kJ/mol
	ΔS	0.130	kJ/mol·K

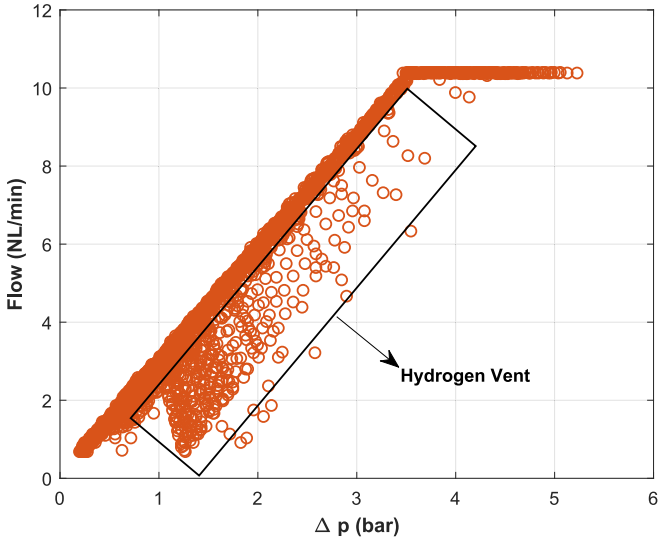

Fig. 5. PEM hydrogen generator flow-Δp characteristic.

The impact of thermal regulation on the hydrogen storage capacity over the test duration is further highlighted in Fig. 7, which presents the temporal evolution of the stored hydrogen mass (in grams) and the system-based wt%$_{ss}$, as previously defined. A 10 °C variation in the thermal set-point results in a final discrepancy of approximately 5 g (600 NL) and 11.4 g (900 NL) of stored hydrogen after 2 h of operation. Notably, at 20 °C, this corresponds to a reduction of approximately 18.5 % (600 NL) and 25 % (900 NL) in the hydrogen uptake, emphasizing the critical role of thermal management in optimizing storage efficiency.

3.2.2. *Impact of the PEM electrolyzer supply pressure*

The difference between the hydrogen supply pressure and the equilibrium pressure of the hydride represents the driving force governing hydrogen diffusion into the metal powder. Consequently, higher feed pressures generate a greater driving force that enhances the hydrogen absorption rate, reducing the duration of the charging phase. This effect is evident in Fig. 8, which compares the results of two tests conducted at 7 bar and 15 bar under the same cooling conditions, with a fluid temperature of 20 °C.

As shown, the hydrogen flow rate decreases as the state of charge of the MH canister increases, further influenced by the temperature rise occurring during the phase of maximum absorption. The charging process, and therefore hydrogen uptake by the storage system, continues until equilibrium is reached between the hydride pressure and the supply pressure. A comparison of Figs. 6 and 8 reveals that the impact of the cooling system on the storage performance is less significant than the effect of supply pressure variation.

This effect is further shown in Fig. 9, which illustrates the temporal evolution of the absorbed hydrogen mass alongside the system-based wt %$_{ss}$. As clearly observed, the variation in supply pressure significantly impacts storage performance. Specifically, reducing the set-point from 15 bar to 7 bar results in a deficit of nearly 20 g of stored hydrogen for the 600 NL tank and over 30 g for the 900 NL tank. These reductions correspond to approximately 74 % and 68 % lower stored quantity, respectively, compared to the optimal condition, highlighting the strong dependence of storage efficiency on supply pressure.

3.2.3. *Scale-dependent considerations for metal hydride absorption dynamics*

The empirical correlations derived from the experimental tests

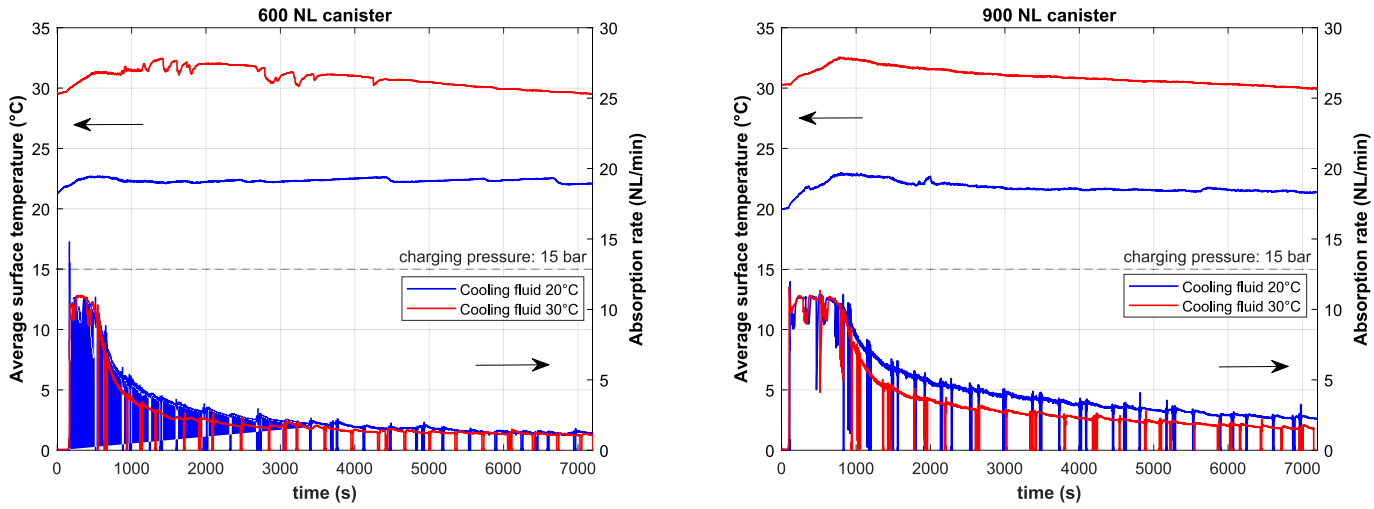

Fig. 6. Average surface temperature and absorption rate for each canister tested (case #3 and #4).

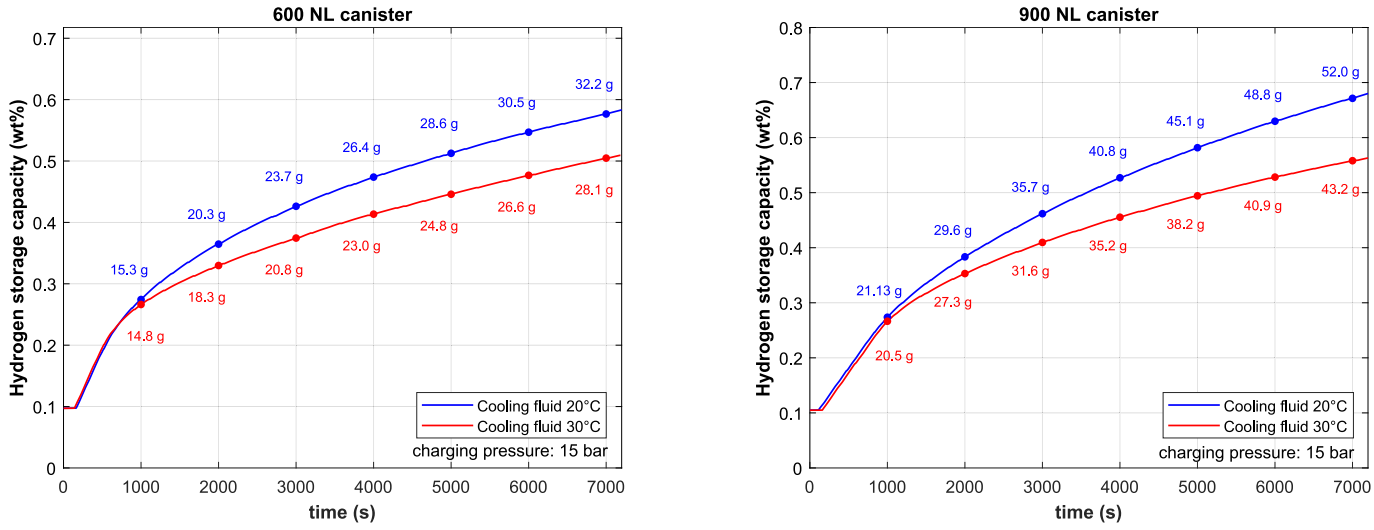

Fig. 7. Evolution of the stored hydrogen mass and wt% for each canister tested (case #3 and #4).

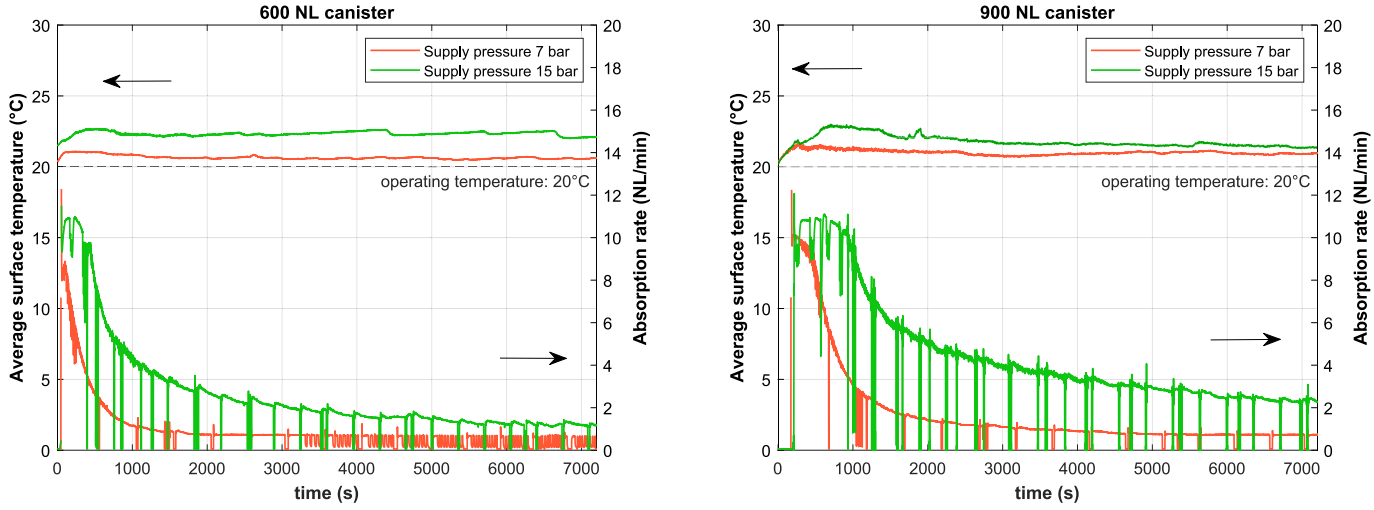

Fig. 8. Average surface temperature and absorption rate for each canister tested (case #1 and #3).

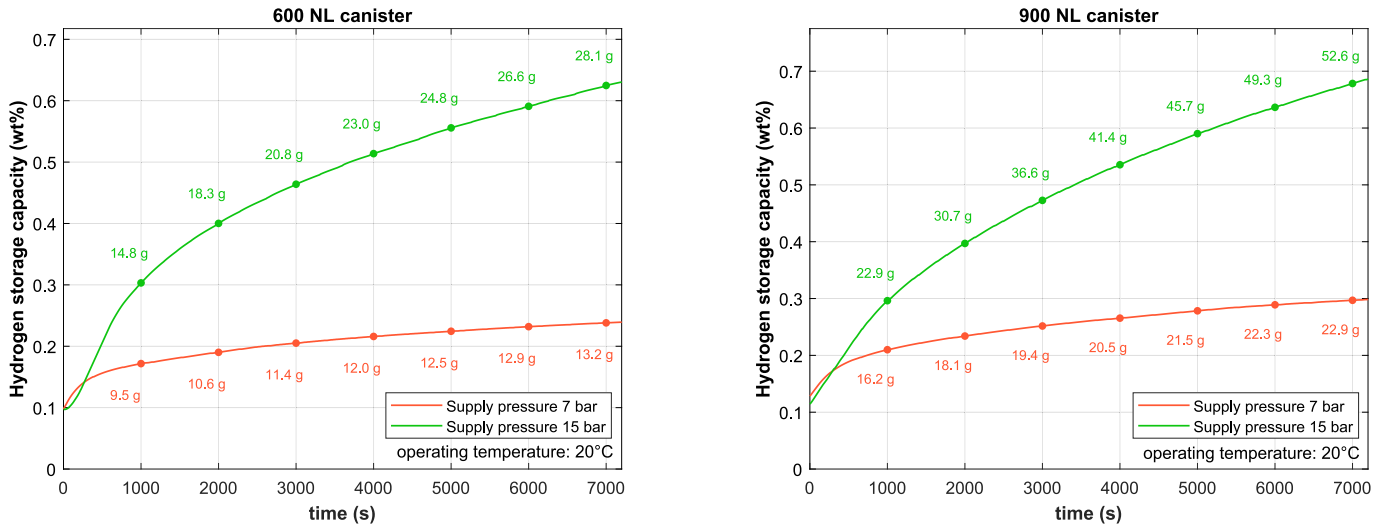

Fig. 9. Evolution of the stored hydrogen mass and wt% for each canister tested (case #1 and #3).

provide valuable insights into the absorption dynamics of MHs. By plotting the absorption rates for both storage tanks as a function of the $wt\%_{ss}$ achieved under optimal conditions (15 bar, 20 °C - Fig. 10), it was observed that the two curves exhibit an identical slope, with the 900 NL tank shifted to the right. At the same time, when expressing the absorption rate as a function of the internal pressure of the storage cylinder, it can be observed that—excluding the effects induced by the hydrogen vent dynamics in the purification line—the general trend of the two curves exhibits comparable absolute values. Notably, the slope of the high-pressure region, which is the most relevant for the analysis, is virtually identical for both system sizes.

These preliminary results suggest that, within the specific devices tested, tank size does not appear to have a significant impact on absorption kinetics, despite a 50 % increase in storage capacity from 600 NL to 900 NL of hydrogen. However, given that the analysis is based on only two devices of different capacities, this observation cannot be generalized. A broader investigation involving a wider range of storage capacities will be necessary to confirm - or revise - this initial indication regarding the influence of tank size in direct coupling configurations with the electrolyzer.

Nevertheless, this result is particularly relevant as it provides a foundation for developing dynamic performance maps of the MH storage system, which could serve as a reference for black-box surrogate models. These models would enable a more accurate and computationally efficient representation of hydrogen absorption behavior in system-level simulations, supporting optimization and control strategies for integrated Power-to-Hydrogen applications.

4. Energy and efficiency analysis

This section presents the energy analysis of the investigated system, carried out following the defined methodology. To support the subsequent discussion, a summary table of the key energy indicators obtained from the analysis is provided below – Table 5.

As reported in the table and illustrated in Figs. 11 and 12, it can be observed that the greatest benefits in terms of overall system efficiency are achieved when operating the plant at higher hydrogen supply pressures (15 bar). In contrast, the introduction of thermal conditioning at 20 °C for the storage system resulted in only a slight improvement in performance under low supply pressure conditions, while it is not advantageous at 15 bar. When examining these scenarios solely from the perspective of storage efficiency, it becomes apparent that adjusting the operational temperature is never a favorable strategy. This is because the energy expenditure associated with thermal conditioning, even

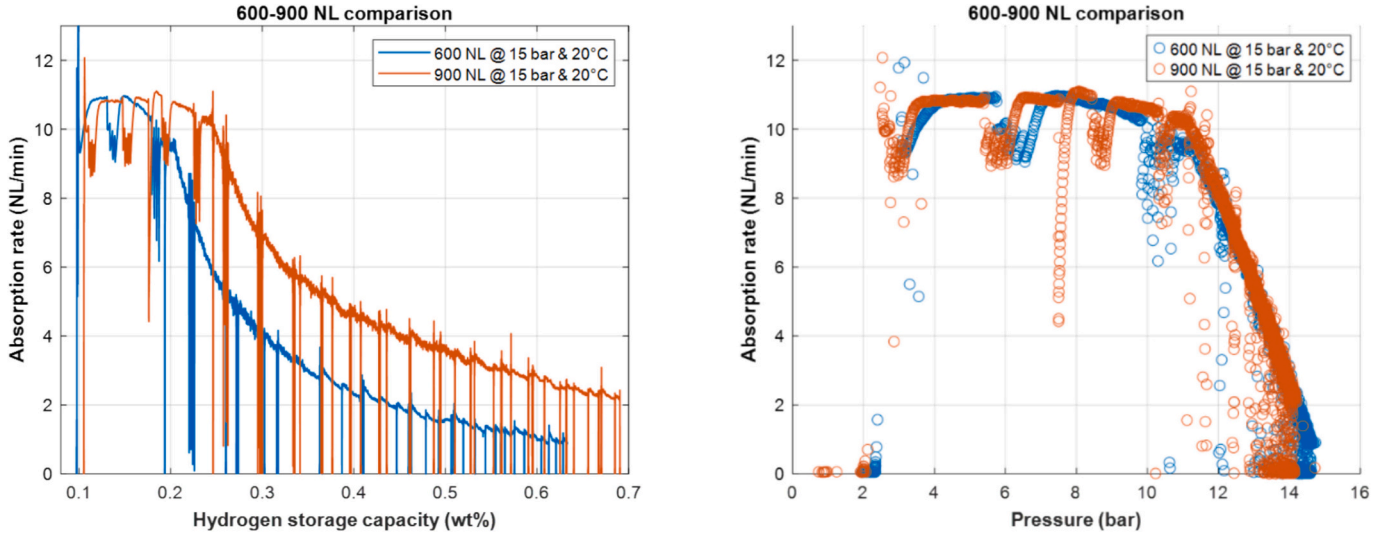

Fig. 10. Absorption rate over wt% (left) and pressure (right) for each canister tested in the best operational conditions (15 bar, 20 °C).

Table 5
Key energy indicators of the investigated P2G.

DoE			Results						
V (NL)	P (bar)	T (°C)	H_2 absorbed (g)	Stack energy consumption (kWh)	Auxiliaries energy consumption (kWh)	Chiller equivalent electricity consumption[a] (kWh)	η_{P2G} (%)	η_{MH} (%)	CF (%)
600	7	20	7.7	0.42	0.41	0.07	27.6	21.3	8.7
	7	30	4.9	0.28	0.33	0.02	25.7	67.1	5.5
	15	20	27.0	1.60	0.43	0.16	41.0	46.6	30.4
	15	30	22.0	1.23	0.43	0.05	43.0	78.4	24.8
900	7	20	14.2	0.76	0.44	0.09	36.5	43.7	16.0
	7	30	9.5	0.54	0.37	0.03	33.5	68.9	10.7
	15	20	44.3	2.47	0.46	0.16	47.8	66.9	49.9
	15	30	32.9	1.75	0.46	0.05	48.3	85.3	37.1

[a] $EER = 3$.

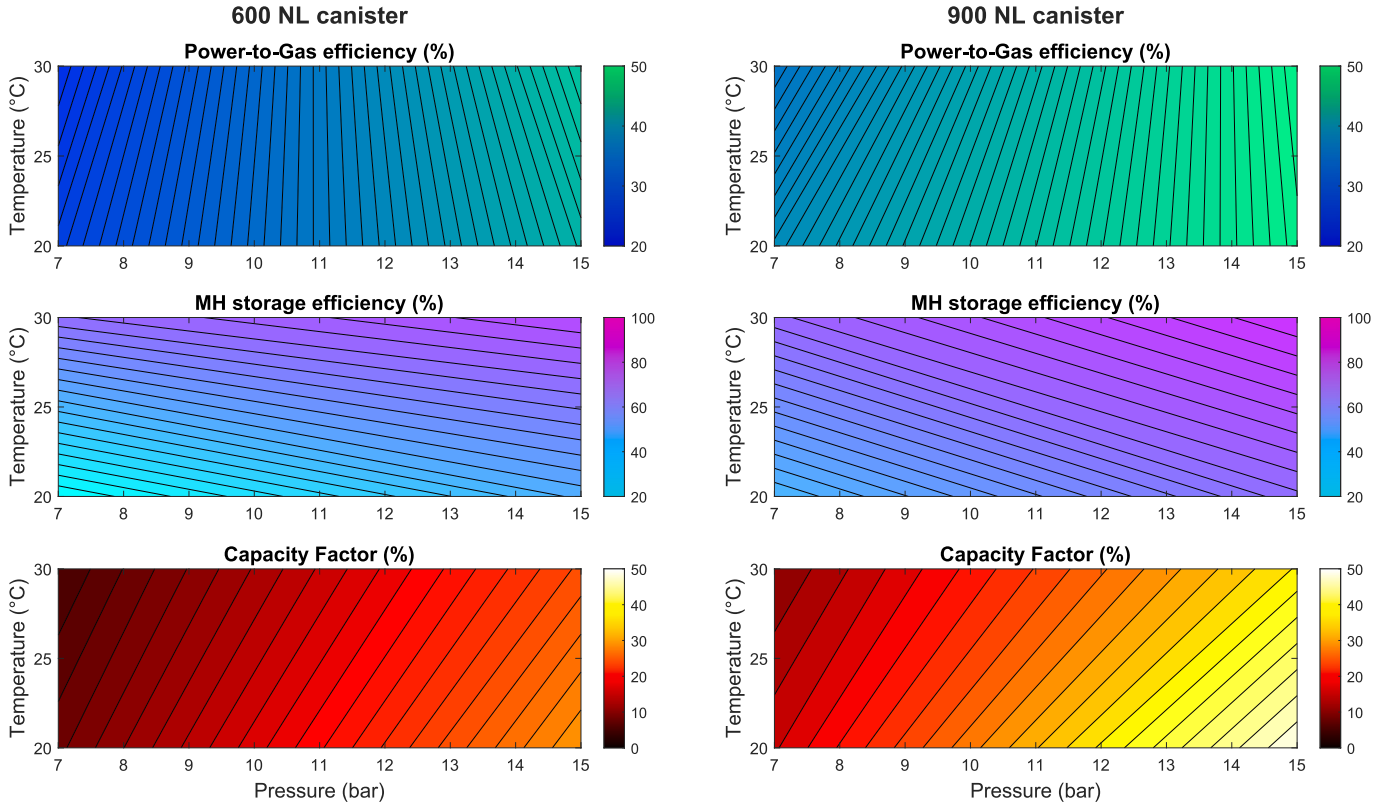

Fig. 11. Performance maps of the system as a function of thermodynamic operating conditions (temperature and pressure).

when not extreme, significantly impacts the overall energy balance, making cooling processes undesirable. It is important to note that the scenarios explored through the DoE were deliberately chosen to closely represent the most likely operating conditions for a real P2G system operating in this configuration. It is well known that enhancing cooling during the charging phase of MHs can benefit the adsorption process; however, the initial approach focused on limiting the thermal conditioning temperature to 20 °C, considering it more as a thermal maintenance strategy rather than a high-performance cooling system, thus excluding lower temperature set-points.

When evaluating the performance of the entire P2G system from the perspective of the capacity factor, it becomes evident that the optimal configuration consistently corresponds to the lowest storage maintenance temperature combined with the highest supply pressure available. This finding, in contrast to the trends observed for system efficiency, indicates that under these conditions, the system is significantly more responsive to the need for maximizing the utilization of excess renewable energy. However, this comes at the expense of a trade-off in operational efficiency, which must be considered when optimizing system performance.

5. Conclusions

This study presents the experimental analysis of a Power-to-Gas (P2G) system composed of a Proton Exchange Membrane (PEM) electrolyzer directly coupled with an AB_2-type metal hydride (MH) storage unit. Given the well-established sensitivity of metal hydrides to pressure and temperature, this study first examined the thermodynamic behavior of a PEM electrolyzer directly coupled with an AB_2-type MH storage unit under varying operating conditions. The system was tested under a range of different pressures and temperatures to evaluate its thermodynamic behavior and energy performance for better integration with an intermittent renewable energy supply. Particular attention was paid to assessing whether the optimal conditions for hydrogen absorption by MH — which turned out to be a high feed pressure (15 bar) and a moderately low storage temperature (~20 °C) — also aligned with improved energy performance at the system level. The energy analysis highlights the trade-off between process efficiency and renewable

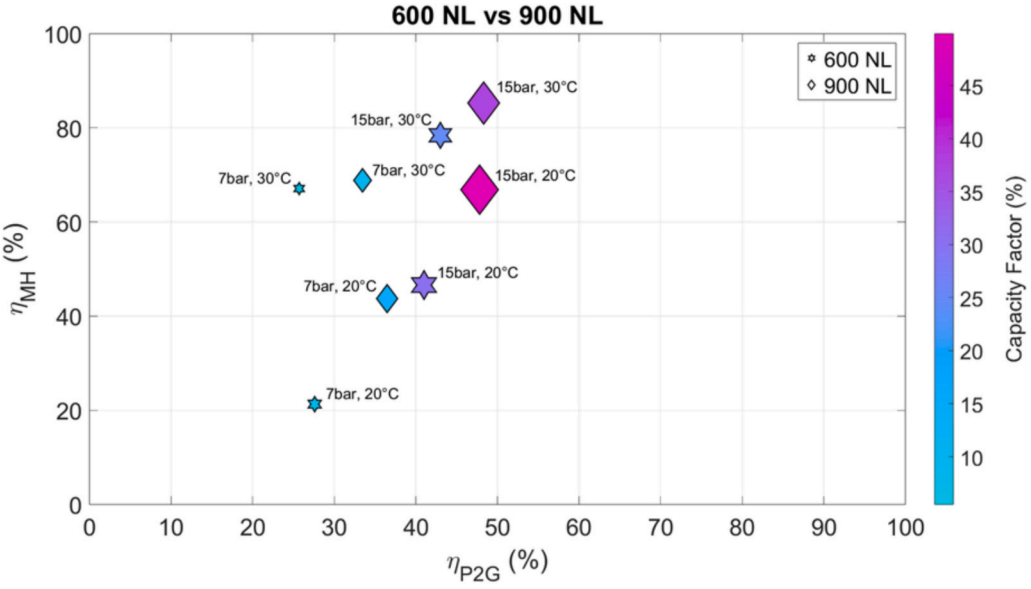

Fig. 12. Comparison of system performance with 600 NL and 900 NL storage capacities.

energy exploitation. On one side, P2G efficiency emphasizes the minimization of energy losses across hydrogen production, absorption, and thermal management. While higher efficiency reflects lower specific energy consumption, it does not necessarily result in maximum hydrogen storage.

On the other side, the capacity factor prioritizes the full utilization of available storage volume, promoting the absorption of as much surplus renewable energy as possible, even at the cost of reduced efficiency. From this perspective, higher supply pressure (15 bar) proves advantageous, as it enables rapid hydrogen absorption, thereby increasing the system's responsiveness and storage utilization.

Based on the combined thermodynamic and energy results, the most advantageous operating point corresponds to the highest tested supply pressure (15 bar) and passive thermal control (maintaining 20 °C without active cooling). This configuration ensures:

- a high capacity factor, enabling maximum capture of renewable energy surplus;
- satisfactory efficiency, with minimal energy losses from cooling;
- a well-balanced system operation, optimizing the trade-off between energy recovery and operational cost.

Ultimately, the choice of operating conditions depends on the intended function of the Power-to-Gas system. In renewable energy integration contexts, maximizing thermodynamic efficiency alone is not sufficient to fully evaluate system performance. Unlike conventional hydrogen production systems, where energy efficiency may be the dominant metric, renewable-driven P2G applications must also prioritize the ability to absorb and store surplus energy that would otherwise be curtailed. From this perspective, the capacity factor, representing the extent to which the storage system can capture and retain the available excess renewable energy, emerges as a critical indicator of overall system effectiveness.

This consideration highlights the inherent trade-off between efficiency and capacity factor. Configurations optimized solely for energy efficiency may underutilize the storage potential during transient peaks in renewable supply, while configurations that favor storage responsiveness - such as operation at higher pressures without active cooling - can improve hydrogen uptake at the expense of slightly higher energy consumption. For this reason, the present study was designed to characterize and compare system behavior under varying conditions, with the specific aim of identifying this trade-off rather than defining a single optimal operating point.

The configuration combining high supply pressure (15 bar) with passive thermal control (~20 °C) was therefore not selected as a universal optimum, but rather as a well-balanced operating point capable of delivering both satisfactory efficiency and high storage utilization under the tested conditions. It is emphasized that the most appropriate operating strategy ultimately depends on the system's objective: whether to minimize energy losses or to maximize renewable energy recovery. Further studies involving a broader range of operating scenarios and storage capacities are necessary to confirm these initial findings and support design choices tailored to specific application goals.

Nomenclature

Acronyms

A	More hydratable element
AC	Alternate Current
B	Less hydratable element
BoP	Balance of Plant
DAQC	Data Acquisition and Control
DC	Direct Current
DoE	Design of Experiment
GUI	Graphic User Interface
HP	High Pressure
LHV	Lower Heating Value
LT	Low Temperature
MH	Metal Hydride
P2H	Power-to-Hydrogen
P2G	Power-to-Gas
P2H2P	Power-to-Hydrogen-to-Power
P2G2P	Power-to-Gas-to-Power
PCT	Pressure Concentration Temperature
PEM	Proton Exchange Membrane
PEM-E	Proton Exchange Membrane Electrolyzer
PLC	Programmable Logic Controller
RES	Renewable Energy Source
SDS	Safety Data Sheet
TRL	Technology Readiness Level

Greek letters

Δ	difference
η	efficiency [−]
ρ	density [kg/m^3]

Symbols

c_l	specific heat [J/kgK]
CF	capacity factor [%]
E	electric energy [kWh]
EER	energy efficiency ratio [−]
H	enthalpy [J]
m	mass [kg]
n	number of moles [mol]
P	power [kW]
p	pressure [bar]
Q	thermal energy [kWh]
R	universal gas constant [J/molK]
S	entropy [J/K]
T	temperature [K] or [°C]
T	time [s]
$\dot{V}$	volumetric flow rate [NL/min]
$wt\%$	weight fraction [%]

Subscripts and superscripts

aux	auxiliary systems
cool	cooling
eq	equilibrium
ss	storage system
th	thermal

CRediT authorship contribution statement

Riccardo Alleori: Writing – review & editing, Writing – original draft, Visualization, Validation, Software, Project administration, Methodology, Investigation, Formal analysis, Data curation, Conceptualization. **Maria Alessandra Ancona:** Writing – review & editing, Supervision, Funding acquisition. **Michele Bianchi:** Writing – review & editing, Supervision, Funding acquisition. **Francesco Falcetelli:** Writing – review & editing, Writing – original draft, Visualization, Validation, Software, Project administration, Methodology, Investigation, Formal analysis, Data curation, Conceptualization. **Federico Ferrari:** Writing – review & editing, Writing – original draft, Visualization, Validation, Software, Project administration, Methodology, Investigation, Formal analysis, Data curation, Conceptualization. **Paolo Pilati:** Writing – review & editing, Writing – original draft, Visualization, Validation, Software, Project administration, Methodology, Investigation, Formal analysis, Data curation, Conceptualization.

Declaration of competing interest

The authors declare that they have no known competing financial interests or personal relationships that could have appeared to influence the work reported in this paper.

Acknowledgements

Funded by European Union - NextGenerationEU - PNRR, M2C2.3.5. Views and opinions expressed are however those of the author(s) only and do not necessarily reflect those of the European Union or of the European Commission or of the Italian Ministry of the Environment and Energy Security. Neither the European Union nor the European Commission nor the Italian Ministry of the Environment and Energy Security can be held responsible for them.

Data availability

Data will be made available on request.

References

[1] N. Klopčič, I. Grimmer, F. Winkler, M. Sartory, A. Trattner, A review on metal hydride materials for hydrogen storage, J. Energy Storage 72 (nov. 2023) 108456, https://doi.org/10.1016/j.est.2023.108456.
[2] J. Bellosta von Colbe, et al., Application of hydrides in hydrogen storage and compression: achievements, outlook and perspectives, Int. J. Hydrogen Energy 44, fasc. 15 (mar. 2019) 7780–7808, https://doi.org/10.1016/j.ijhydene.2019.01.104.
[3] Schneemann, et al., Nanostructured metal hydrides for hydrogen storage, Chem. Rev. 118, fasc. 22 (nov. 2018) 10775–10839, https://doi.org/10.1021/acs.chemrev.8b00313.
[4] S.S. Bhogilla, Design of a AB2-metal hydride cylindrical tank for renewable energy storage, J. Energy Storage 14 (2017) 203–210, https://doi.org/10.1016/j.est.2017.10.012.
[5] V.K. Sharma, Anil Kumar, Metal hydrides for energy applications – classification, PCI characterisation and simulation, Int. J. Energy Res. 41, fasc. 7 (2017) 901–923, https://doi.org/10.1002/er.3668.
[6] J.B. Von Colbe, J.R. Ares, J. Barale, M. Baricco, C. Buckley, G. Capurso, M. Dornheim, Application of hydrides in hydrogen storage and compression: achievements, outlook and perspectives, Int. J. Hydrogen Energy 44 (15) (2019) 7780–7808, https://doi.org/10.1016/j.ijhydene.2019.01.104.
[7] M.V. Lototskyy, V.A. Yartys, B.G. Pollet, R.C. Bowman Jr., Metal hydride hydrogen compressors: a review, Int. J. Hydrogen Energy 39 (11) (2014) 5818–5851, https://doi.org/10.1016/j.ijhydene.2014.01.158.
[8] C. Drawer, J. Lange, M. Kaltschmitt, Metal hydrides for hydrogen storage – Identification and evaluation of stationary and transportation applications, J. Energy Storage 77 (2024) 109988 gen, https://doi.org/10.1016/j.est.2023.109988.
[9] X. Wang, P. Peng, M. Witman, V. Stavila, M. Allendorf, H. Breunig, Technoeconomic insights into metal hydrides for stationary hydrogen storage, ChemRxiv (3 ottobre 2024), https://doi.org/10.26434/chemrxiv-2024-gwrzq.
[10] M.V. Lototskyy, B.P. Tarasov, V.A. Yartys, Gas-phase applications of metal hydrides, J. Energy Storage 72 (2023) 108165, nov, https://doi.org/10.1016/j.est.2023.108165.
[11] F. Franke, S. Kazula, Evaluation of the potential of metal hydride applications in future hydrogen-powered aviation, in: 2023 IEEE Transportation Electrification Conference & Expo (ITEC), 2023, pp. 1–8, https://doi.org/10.1109/ITEC55900.2023.10186988, giu.
[12] Hauch, et al., Recent advances in solid oxide cell technology for electrolysis, Science 370, fasc. 6513 (2020), https://doi.org/10.1126/science.aba6118 p. eaba6118, ott.
[13] M. Bielmann, U.F. Vogt, M. Zimmermann, A. Züttel, Seasonal energy storage system based on hydrogen for self sufficient living, J. Power Sources 196 (8) (2011) 4054–4060, https://doi.org/10.1016/j.jpowsour.2010.11.096.
[14] P. Rizzi, E. Pinatel, C. Luetto, P. Florian, A. Graizzaro, S. Gagliano, M. Baricco, Integration of a PEM fuel cell with a metal hydride tank for stationary applications, J. Alloys Compd. 645 (2015) S338–S342, https://doi.org/10.1016/j.jallcom.2014.12.145.
[15] E.M. Dematteis, J. Barale, M. Costamagna, P. Rizzi, M. Baricco, C. Makhloufi, M. Latroche, HyCARE: Hydrogen Carrier for Renewable Energy Storage. https://sciforum.net/paper/view/8955, 2021.
[16] N. Gallandat, J. Bérard, F. Abbet, A. Züttel, Small-scale demonstration of the conversion of renewable energy to synthetic hydrocarbons, Sustain. Energy Fuels 1 (8) (2017) 1748–1758, https://doi.org/10.1039/c7se00275k.
[17] P.C. Rodriguez, N. Gallandat, A. Züttel, Accurate measurement of pressure-composition isotherms and determination of thermodynamic and kinetic parameters of metal hydrides, Int. J. Hydrogen Energy 44 (26) (2019) 13583–13591, https://doi.org/10.1016/j.ijhydene.2019.03.224.
[18] M. Lototskyy, B.S. Sekhar, P. Muthukumar, V. Linkov, B.G. Pollet, Niche applications of metal hydrides and related thermal management issues, J. Alloys Compd. 645 (2015) S117–S122, https://doi.org/10.1016/j.jallcom.2014.12.271.
[19] Electric Generator Capacity Factors Vary Widely Across the World, U.S. Energy Information Administration (EIA), 2015. https://www.eia.gov/todayinenergy/detail.php?id=22832.